Physical characterization, magnetic measurements, REE geochemistry and biomonitoring of dust load accumulated during a protracted winter fog period and their implications

Munmun Chakarvorty, Jayanta Kumar Pati, Shiva Kumar Patil, Swati Shukla, Ambalika Niyogi & Arun Kumar Saraf

Environmental Monitoring and Assessment
An International Journal Devoted to Progress in the Use of Monitoring Data in Assessing Environmental Risks to Man and the Environment

ISSN 0167-6369
Volume 186
Number 5

Environ Monit Assess (2014)
186:2965-2978
DOI 10.1007/s10661-013-3594-4

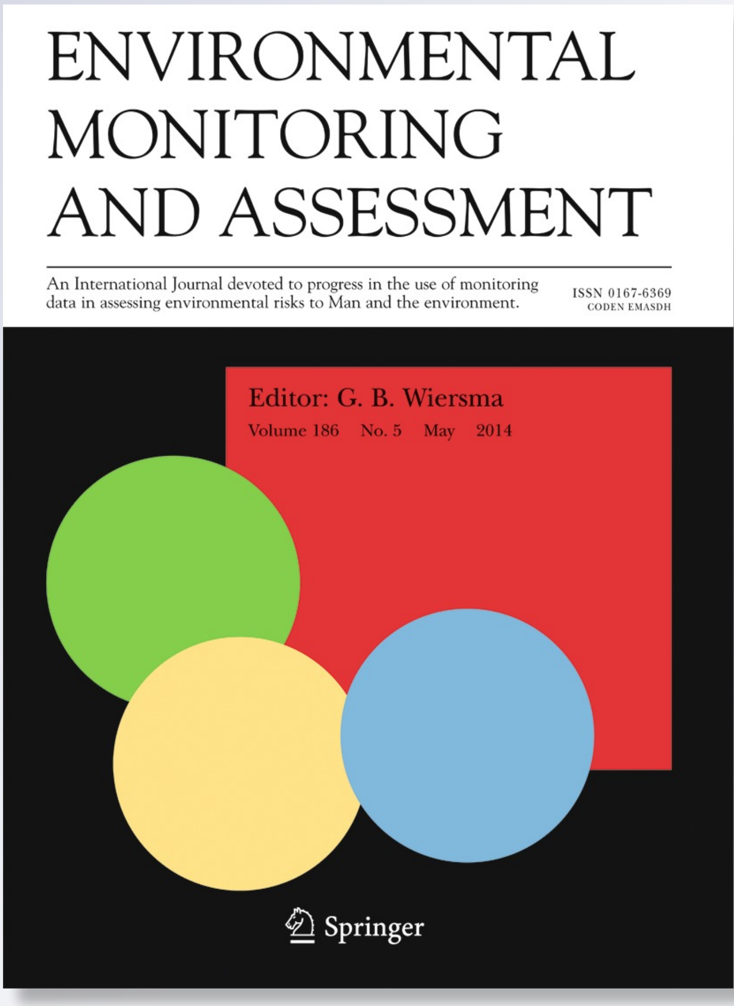

Springer

Environ Monit Assess (2014) 186:2965–2978
DOI 10.1007/s10661-013-3594-4

Physical characterization, magnetic measurements, REE geochemistry and biomonitoring of dust load accumulated during a protracted winter fog period and their implications

Munmun Chakarvorty · Jayanta Kumar Pati · Shiva Kumar Patil · Swati Shukla · Ambalika Niyogi · Arun Kumar Saraf

Received: 29 January 2013 / Accepted: 23 December 2013 / Published online: 10 January 2014

Abstract The winter fog in India is a recurrent phenomenon for more than a decade now affecting the entire Himalayan and sub-Himalayan regions covering an area of nearly 500,000 km^2. Every winter (December–January), the air and surface transports in cities of northern India (Amritsar, New Delhi, Agra, Gwalior, Kanpur, Lucknow, and Allahabad) are severely disrupted with visibility reduced to <50 m at times. Since dust particles are known to act as nuclei for the fog formation, this study is aimed to carry out physicochemical characterization of the dust particulates accumulated during a protracted fog period from one of the severely fog affected cities of north India (Allahabad; 25°27′33.40″N–81°52′45.47″E). The dust-loaded tree leaves belonging to *Ficus bengalensis* and *Ficus religiosa* from 50 different locations between January 24 and 31, 2010 are sampled and characterized. The mass of dust, color, grain shape, size, phase constituents, and mineral magnetic parameters, such as magnetic susceptibility, SIRM, χ_{fd}%, and *S*-ratio, show minor variation and the regional influence outweighs local anthropogenic contributions. The dust compositions show fractionated rare earth element pattern with a pronounced negative Eu anomaly similar to upper continental crust and further suggesting their derivation from sources located in parts of north and central India.

M. Chakarvorty · J. K. Pati (✉) · S. Shukla · A. Niyogi
Department of Earth and Planetary Sciences, University of Allahabad, Allahabad 211 002, India
e-mail: jkpati@gmail.com

S. K. Patil
Dr. K.S. Krishnan Geomagnetic Research Laboratory, Leelapur Road, Hanumanganj, Allahabad 221 505, India

A. K. Saraf
Department of Earth Sciences, Indian Institute of Technology, Roorkee, Uttarakhand 247667, India

Keywords Physical characterization · Magnetic susceptibility · Particulate matter · Winter fog · Biomonitoring

Introduction

Fog disrupts surface and air transport in the entire northern India between the months of November and January every year (Ali et al. 2004; Prasad & Singh 2007; Singh et al. 2011; Jenamani & Tyagi 2011; Saraf et al. 2011; Tiwari et al. 2011) and similar conditions are observed in other parts of the world as well (Biswas et al. 2008; Cereceda et al. 2008). In India, so far, the studies have been confined to the analysis of fog water (Ali et al. 2004), anthropogenic causes of fog formation (Prasad & Singh 2007; Choudhury et al. 2007), monitoring (Jenamani & Tyagi 2011) and spatio-temporal variation of fog pattern (Saraf et al. 2011), experimental study pertaining fog formation and dissipation (Singh et al. 2011), and algorithm development for night time fog detection (Chaurasia et al. 2011). Saraf et al. (2011) studied the winter fog pattern observed in Indo-Gangetic plains between 2005 and 2008 using remote sensing and geographic information system (GIS) techniques. They observed that the fog in Indo-Gangetic plains has varied significantly during 2005–

2008 [575,800 km^2 (2005–2006), 594,100 km^2 (2006–2007), and 478,000 km^2 (2007–2008)] and further attributed that such variations may be the consequence of high fluctuations in the meteorological parameters prevailed in the area.

This study has been carried out in parts of Allahabad City, north central India for the first time to study the dust load accumulated during a dense fog period observed in the month of January 2010 (Chaurasia et al. 2011) pertaining to their physical properties (absolute mass of the dust load, color, grain size, particulate shape, and phase characterization), magnetic properties, rare earth element (REE) geochemistry of the dust load, and biomonitoring using two well-known natural sinks (*Ficus bengalensis* and *Ficus religiosa*). The objective of the present study is to physicochemically characterize the dust matter collected during a winter fog period in north India and link the sink particulate to its possible source.

Materials and methods

Study area

The city of Allahabad spread over 70 km^2 area is located in the northern Indian state of Uttar Pradesh and is a famous centre of pilgrimage with a population of 1,206,785 inhabitants (2001 Census; http://en.wikipedia.org/wiki/Allahabad; December 20, 2011) 21 and Yamuna rivers and at an elevation of 98 m from the mean sea level. Of the nine major cities of north India affected by winter fog, the least numbers of industries are located in Allahabad. The city experiences a humid subtropical climate, common to cities in north-central India. Allahabad witnesses mainly three seasons: hot dry summer, cool dry winter, and warm humid monsoon. The summer season lasts from April to June with the maximum temperatures ranging from 40 to 47 °C. Monsoon begins in early July and lasts till September. The Allahabad City receives an average rainfall of about 97 cm year^{-1}. The winter season lasts from December to February with the minimum and maximum temperatures between 3 and 22 °C, respectively. Like all major cities in the north India occurring in the foreland basin, Allahabad experiences dense fog between December and January every year (Saraf et al. 2011) disrupting surface and air transports severely.

Sampling

Various types of particle collectors are employed for the sampling of the fog-related particulate matter. The road-side tree leaves are one of them and known as better sinks for the collection of large number of samples (Gautam et al. 2005). This biomonitoring tool has been used extensively in various thematic studies involving atmospheric aerosols (Gautam et al. 2005; Lorenzini et al. 2006; Prajapati & Tripathi 2008; Maher et al. 2007; Power et al. 2009; Tomaˇsevi'c et al. 2005), mineralogical characterization of the particulate matter (Charlesworth & Lees 1997; Abdul-Razzaq & Gautam 2001), geochemical analysis of dust load (Petrovsky & Ellwood 1999; Hanesch & Scholger 2002; Muxworthy et al. 2002; Wong et al. 2006; Lu et al. 2008; Yang & Chen 2002), and magnetic measurements (Blaha et al. 2008; Lu et al. 2007; Shu et al. 2000; Goddu et al. 2004; Flanders 1994; Gautam et al. 2005; Hoffmann et al. 1999; Maher et al. 2007; Moreno et al. 2003; Hanesch et al. 2003; Oldfield et al. 1985). The road-side tree leaves are also considered as extremely suitable to access and monitor the source of particulate matter (Chen et al. 1999; Spassov etal. 2004) and to ascertain their spatio-temporal distribution pattern.

The dust samples were collected from 50 representative locations close to various roads within Allahabad City, India (Fig. 1) from two species of deciduous *Ficus* trees (*F. bengalensis* and *F. religiosa*) with sampling confined to branches facing the road and at a height of 2–2.5 m above ground level. Each sample represents total mass of particulate matter collected from ten morphologically identical dust-loaded *Ficus* leaves. The dust samples were stored in precleaned plastic dust collectors of known magnetic susceptibility and preserved at ambient temperature. The color, leaf area, leaf weight, and mass of the dust (Fig. 2; Table 1) were observed in each case. The sampling was carried out between January 24 and 30, 2010 during a marked fog (Fig. 3) phase preceded by a bout of heavy to moderate rain fall on January 21, 2010. The leaf dust samples were collected 3 days after the rainfall assuming total washout of the pre-rain dust load and further suggesting the collected dust samples to representative of the fog phase.

Grain size analysis

The SEM and BSE-SEM images of five representative dust samples (Nos. 6, 20, 28, 36 and 44) are obtained

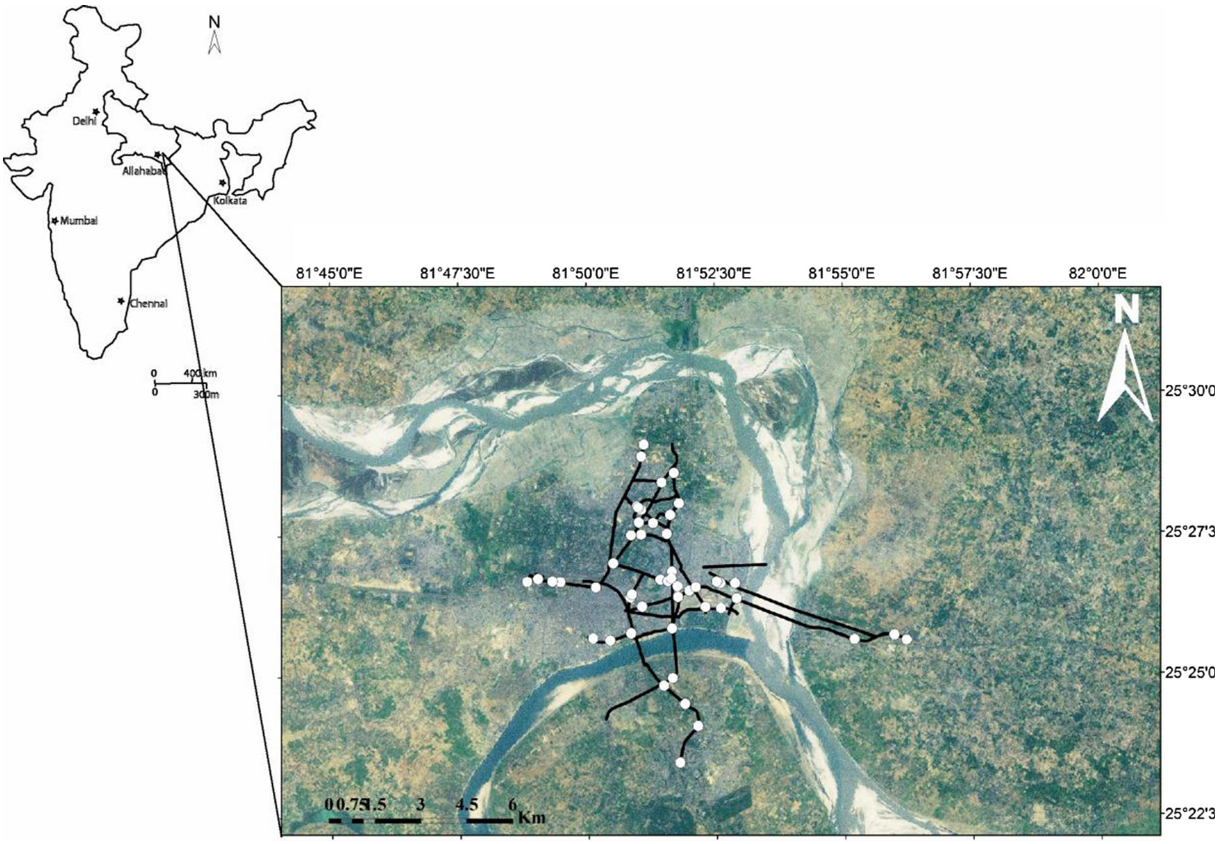

Fig. 1 Schematic map of the India showing the state boundary of Uttar Pradesh and Allahabad City, the study area is shown in GoogleEarth® image, *white filled circles* are sampling points and *black lines* are road networks

using an electron probe micro analyzer (EPMA; Cameca SX 100, PLANEX, Physical Research Laboratory, Ahmedabad) for grain size and particle shape analyses. The samples were vacuum-coated in gold and imaged using scanning electron microscopy (SEM) mode. The BSE technique is used in order to evaluate phase contrast in dust particulate matter. The semiquantitative analyses of the dust load are made to identify various phases present. The error in grain size measurement is better than 5 %.

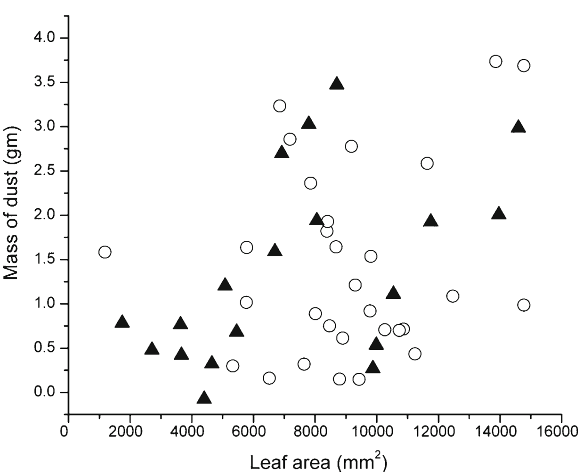

Fig. 2 Relation between the leaf area (mm^2) (*Open circles*: *Ficus bengalensis*; *Filled triangles*: *Ficus religiosa*) vs. mass of dust (g) showing a faint positive correlation

X-ray diffraction

Mineralogy of the dust was determined by X-ray diffraction (XRD) analysis with non-oriented powder X-ray diffractometer (Pan Analytical) with a Cu K$\acute{\alpha}$ radiation. Analytical conditions for all samples scans were conducted from 10 to 64 at a rate of 2° min^{-1} divergence slit = 1°, antiscatter slit = 1°, receiving slit = 0.30 mm, generator voltage= 40 kV, tube current = 30 mA, and scanning speed–2° 2θ min^{-1}.

Table 1 The mass of dust, their color, grain shape, leaf type and leaf area for five representative leaf dust samples are summarized

Sample	Sample no.	Location: Latitude (N°)	Location: Longitude (E°)	Location: Elevation (m)	Physically derived from place	Tree type	Amount of dust (mass of dust per ten leaves) (g)	Color of dust (Munshell color chart®)	Grain shape (%)	Leaf area (mm^2)
1	6	25°26′23.7″ N	81°51′45.8″ E	50±3	National Highway Baihrana (near Power House)	*Ficus bengalensis*	1.0166	Olive gray 5YR 4/1	Needle shape 0.69, subrounded 41.24	5,768
2	20	25°26′30.3″ N	81°51′58.9″ E	80±7	Tularambagh Crossing (near Sabzi Mandi)	*F. bengalensis*	3.7357	Light olive gray 5YR 5/2	Needle shape 0.52 subrounded 40.94	1,386
3	28	25°25′37.7″ N	81°55′11.9″ E	86±3	Chack Jhunsi (in front of Allahabad Bank)	*F. bengalensis*	3.6892	Pale yellowish brown 10 YR 6/2	Needle shape 1.82, subrounded 43.15	14,770
4	36	25°26′40.5vN	81°48′49.4″E	93±3	Lukerganj (near Flour Mill Company)	*Ficus religiosa*	0.9021	Light olive gray 5YR 5/2	Needle shape 3.6, subrounded 43.17	6,212
5	44	25°29′05.9″ N	81°51′06.8″E	84±4	Beli Road (Cantonment Area)	*F. religiosa*	0.2949	Olive gray 5YR 4/1	Needle shape 1.5, subrounded 38.86	4,869

Magnetic measurements of particulate matter

The dust samples were weighed on Mettler (Germany) electronic balance and the magnetic susceptibility of dust samples was measured (in SI unit) using a dual frequency (0.47 and 4.7 kHz) magnetic susceptibility meter (MS2B; Bartington, UK). Susceptibility measurements are made within 24 h of their collection to preserve their natural moisture. The frequency-dependent magnetic susceptibility (χ_{fd}%) was also calculated. All magnetic measurements except the magnetic susceptibility are made using the facilities available in Dr. K.S. Krishnan Geomagnetic Research Laboratory (Government of India), Allahabad. The Molspin pulse magnetizer and Molspin spinner magnetometer are used for isothermal remanent magnetization (IRM) experiments. The saturation induced remanent magnetization (SIRM) and *S*-ratios were calculated by using the formula given by Bloemendal et al. (1992) and noted in Table 2. The χ_{fd}% reflects the relative importance of ferromagnetic grains close to superparamagnetic (SP)/single domain (SD) and SIRM/χ_{lf} may be used as an indicator of the fine-grain (diameter < 1.4 μm) magnetic minerals (Dunlop 1973). Magnetic susceptibility depends on the whole composition of the dust deposited on the leaves and is, however, dominated by ferromagnetic minerals that have much higher susceptibility values than other common paramagnetic and diamagnetic minerals like clay or quartz (Moreno et al. 2003).

REE analyses

The REE geochemistry of ten representative dust samples showing variable magnetic susceptibility is investigated using inductively coupled plasma-mass spectrometry (ICP-MS, Varian) technique (Chemical Division, Geological Survey of India, Lucknow). Approximately 0.1 g of each sample is digested by 8 ml aqua regia in a microwave oven (Mars-5; CEM, USA). After digestion, the solution is filtered and diluted with deionized water to get 50 ml of solution and the elemental concentrations of La, Ce, Pr, Nd, Pm, Sm, Eu, Gd, Tb, Dy, Ho, Er, Tm, Yb, and Lu are determined by ICP-MS and GSD-10 was used as internal standard.

Statistical analysis

For all the measurements, the rank, mean, and standard deviation are calculated. The correlation coefficients

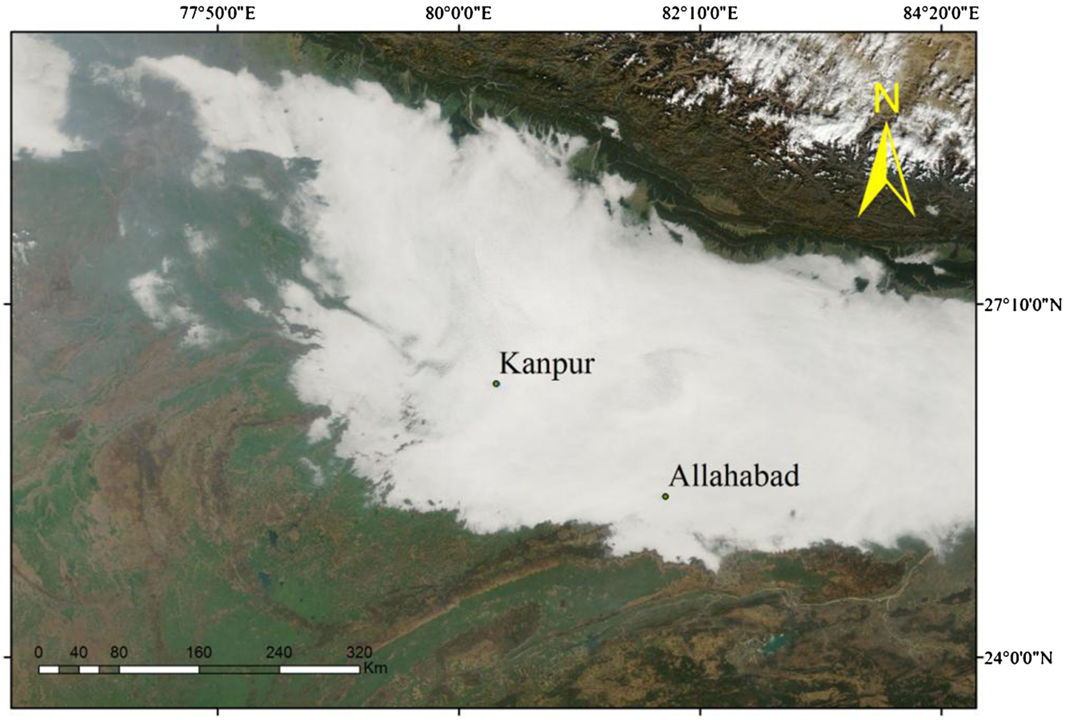

Fig. 3 Satellite Aeronet MODIS terra map showing dense fog observed on second day (January 25, 2010) of the sampling period in parts of northern India (http://IITRoorkee/IITRoorkee; December 20, 2012)

are calculated in order to establish relationship between mass of the dust load and leaf area. Two- and three-dimensional spatial variation maps of magnetic parameters are prepared using ArcGIS® (v.10) and ArcInfo® (v.10) softwares.

Results and discussion

Physical properties of dust

The sample locations in parts of Allahabad City, India and the sample weights are given in Table 3. The bulk weight of the accumulated dust load is variable and they

Table 2 Measurements pertaining to various magnetic parameters, such as χ_{lf}, SIRM χ_{fd}%, χARM, *S*-ratio % of leaf dust samples from the study area are summarized

Measurements	Units	Range	Mean
χ_{lf}	10^{-8} m^3 kg^{-1}	16.09–214.5	125.9
χ_{fd}%	%	0–14.11	6.834
SIRM	10^{-5}A m^2 kg^{-1}	928.69–9,614.687	5,231.939
S-ratio	%	83.28–100	94.894

range from 0.10 to 3.74 g ($\overline{X}$ =1.12; SD=0.93; Table 3). The two chosen biomonitoring sinks (*F. bengalensis* and *F. religiosa*) show variable dust load (0.1473–3.7357 g and 0.0957–1.5155 g, respectively). In general, the leaf area is known to be directly proportional to the amount of accumulated dust (Fig. 2). The measured leaf area of *F. bengalensis* ranges between 14,771.70 and 1,182.65 mm^2 ($\overline{X}$ =9,142.34 mm^2) which is more than *F. religiosa* (13,067.24–3,427.78 mm^2; $\overline{X}$ = 7,655.23 mm^2). In addition to leaf area, the mass of the dust in tree leaves increases with traffic density. The color of the leaf dust collected during the present study is observed to vary from sample to sample, and it is dependent on phase constituents and their physico-chemical properties. A systematic study of dust color has been made by comparing with the standard Geological Society of America Color Chart (Munshell Color Chart®) and it varies between brown (pale yellowish brown 10 YR 6/2 and dark yellowish brown 10 YR 4/2) and dark grey (yellowish grey 5YR, 7/2 to light olive grey 5YR, 5/2). The present study suggests that the color of dust is dependent upon source characteristics. For example, the pale yellowish brown 10 YR 6/2 to dark yellowish brown 10 YR 4/2 dust has a proximal

Table 3 Description of sampling locations from different parts of Allahabad City, India

Sample no.	Place	Latitude (N°)	Longitude (E°)	Weight of dust sample (g)
1	Trans New Yamuna Bridge (Crossing)	25°24′49.3″N	81°51′28.6″E	0.5426
2	Arail Turning, Naini (Tricrossing)	25°24′06.2″N	81°52′08.4″E	0.3178
3	Mewa Lal Baghia, Naini near Station Road (Tricrossing)	25°23′27.2″N	81°51′47.3″E	2.8578
4	Central Jail, Naini (Tricrossing)	25°24′29.9″N	81°51′53.4″E	0.0957
5	New Yamuna Bridge, Naini near Toll Tax Office	25°24′57.4″N	81°51′38.9″E	0.2991
6	National Highway, Baiharana near Power House	25°26′23.7″N	81°51′45.8″E	1.0166
7	Bai Ka Bagh (Crossing)	25°26′13.5″N	81°51′03.8″E	3.2333
8	Nehru Science Centre Gate, University of Allahabad	25°27′30.1″N	81°51′03.1″E	0.7618
9	Sumitra Nandan Pant Children's Park Gate (Elephant Park)	25°27′29.6″N	81°50′51.1″E	0.9288
10	Hanumat Niketan, Civil Lines	25°26′59.7″N	81°50′30.1″E	0.4319
11	Hanuman Mandir, Rambagh (Crossing)	25°26′23.5″N	81°50′50.2″E	0.8957
12	Rambagh near Railway Crossing	25°26′26.5″N	81°50′51.8″E	1.8189
13	Bank Road (Tricrossing)	25°25′50.1″N	81°51′38.6″E	1.3198
14	M. G. Marg in front of K. P. Inter College	25°26′42.2″N	81°51′25.3″E	0.6138
15	C.M.P. Degree College (Tricrossing)	25°26′40.5″N	81°51′34.1″E	1.9295
16	George Town	25°26′50.5″N	81°51′38.6″E	0.4390
17	George Town	25°26′50.5″N	81°51′38.6″E	1.5841
18	Malaviya Road George Town	25°26′43.3″N	81°51′38.1″E	1.6430
19	In front of Bharat Shevashram Sangh, Tularambagh	25°26′35.1″N	81°51′45.1″E	0.8887
20	Tularambagh Crossing near Sabzi Mandi	25°26′30.3″N	81°51′58.9″E	3.7357
21	Fort Road Pared Ground (Tricrossing)	25°26′12.9″N	81°52′17.7″E	0.4351
22	Triveni Road Kumbh Mela Region	25°26′11.5″N	81°52′35.8″E	1.2116
23	Daraganj Bandh Road	25°26′21.9″N	81°52′54.4″E	0.9189
24	Daraganj Tricrossing near Railway Station	25°26′38.0″N	81°52′52.6″E	0.2557
25	Alopibagh (Tricrossing)	25°26′38.1″N	81°52′35.2″E	1.0860
26	Sardar Patel Tricrossing Baghmbri Road, Allahapur	25°26′39.7″N	81°52′31.2″E	2.7765
27	Shastri Bridge, Chungi	25°26′33.9″N	81°52′06.7″E	1.5360
28	Chack Jhunsi in front of Allahabad Bank	25°25′37.7″N	81°55′11.9″E	3.6892
29	Andava Bypaas, Jhunsi	25°25′42.4″N	81°55′58.9″E	1.3372
30	Andava Turning, Jhunsi	25°25′36.9″N	81°56′12.9″E	0.7504
31	Katghar (Crossing)	25°25′37.9″N	81°50′26.1″E	0.9856
32	Dariyabad Police Chauki	25°25′40.0″N	81°50′06.1″E	0.1473
33	Johnstonganj (Crossing)	25°26′34.1″N	81°50′09.6″E	1.2048
34	Railway Station, Leader Road in front of V.I.P. Gate	25°26′40.0″N	81°49′28.1″E	0.3985
35	Lukerganj near Aaj Press	25°26′43.5″N	81°49′01.9″E	0.7143
36	Lukerganj near Flour Mill	25°26′40.5″N	81°48′49.4″E	0.9021
37	Khusru Bagh Gateway, Leader Road	25°26′40.8″N	81°49′18.8″E	1.5155
38	Manmohan Park (Crossing)	25°27′43.3″N	81°51′00.3″E	0.1505
39	Gate of Science Faculty, University of Allahabad	25°27′42.5″N	81°51′16.9″E	0.7069
40	Gaughat Fish Market (Crossing)	25°25′45.2″N	81°50′50.7″E	2.5858
41	Netram Crossing, Katra	25°27′56.9″N	81°51′03.0″E	0.6070
42	Katchery Road, Katra	25°28′00.3″N	81°50′58.0″E	0.1604
43	Auto Stand, Katra	25°27′59.1″N	81°50′59.5″E	0.2346
44	Beli Road, Cantonment Area	25°29′05.9″N	81°51′06.8″E	0.2949

Table 3 (continued)

Sample no.	Place	Latitude (N°)	Longitude (E°)	Weight of dust sample (g)
45	Noorabad Drain, Beli Road (Pulia)	25°28′53.2″N	81°51′03.6″E	1.6359
46	Lala Lajpat Rai Road Mumfordganj in front of Master Zahurul Hasan Road	25°28′25.5″N	81°51′27.3″E	0.3189
47	Near Bharat Scouts and Guide School in front of Ganga Vihar	25°28′35.5″N	81°51′41.8″E	0.7000
48	Lalla Ki Chungi near Women Hostel	25°28′3.31″N	81°51′47.5″E	0.5703
49	University of Allahabad Arts faculty Gate (K.P.U.C. Side)	25°27″50.9″N	81°51′37.0″E	0.3406
50	In front of Anand Bhawan, M. G. Marg	25°27′30.9″N	81°51′33.1″E	2.3622

alluvium/crustal source. However, the dust color varies from yellowish grey 5YR, 7/2 to light olive grey 5YR, 5/2 in traffic congested and industrial areas, respectively. The size of 1,811 individual dust particles varies from 1.5 to 100 μm (Table 1; Figs. 4 and 5). The particle size was measured using five BSE images covering 2,600× 2,000 μm^2 area in each case. It is interesting to note that 59.08 % of the grains fall within the well-established fog particulate size range (0.23 and 20 μm; Pant et al. 2010). Nearly 75 % of the grains measure between 1 and 40 μm and about 24 % to 34 % of the grains occur within PM_{10} and $PM_{1.5}$. The BSE-SEM images of the dust particles show variable shapes (subrounded, rounded, well-rounded, angular and acicular; Fig. 4). The most dominant particle shape is subrounded (35.92 %) followed by rounded (23.56 %), angular (28.97 %), well-rounded (6.78 %), and acicular (3.09 %). The shapes of about 1.68 % particles could not be analyzed due to blurred portions.

X-ray diffraction

The XRD patterns of the dust samples are identical and only three representative spectra are shown in Fig. 6. The analyses reveal the presence of feldspar, quartz, mica, ilmenite, calcite, albite, and muscovite. The relative peak intensities and respective position (2θ) of various phases present in the samples are also similar, suggesting their identical composition and modal volume in respective samples.

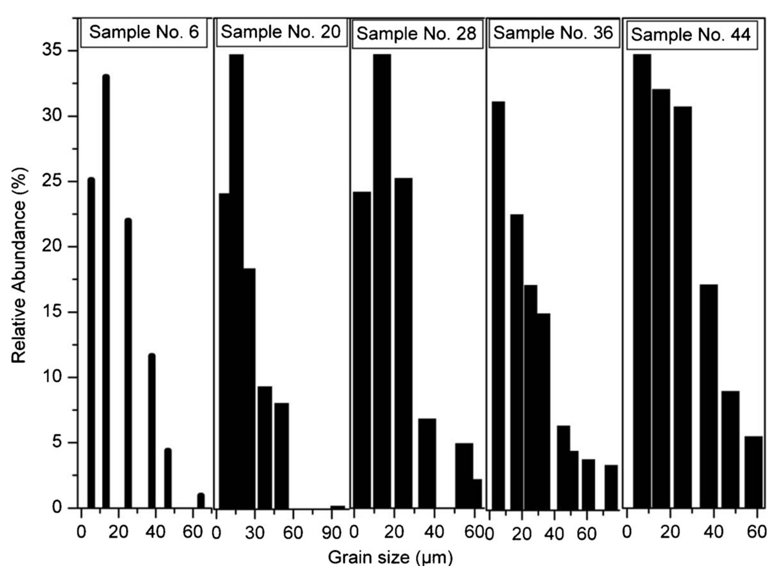

Fig. 4 The plot between relative abundance vs. grain size of leaf dust shows a polymodal distribution pattern

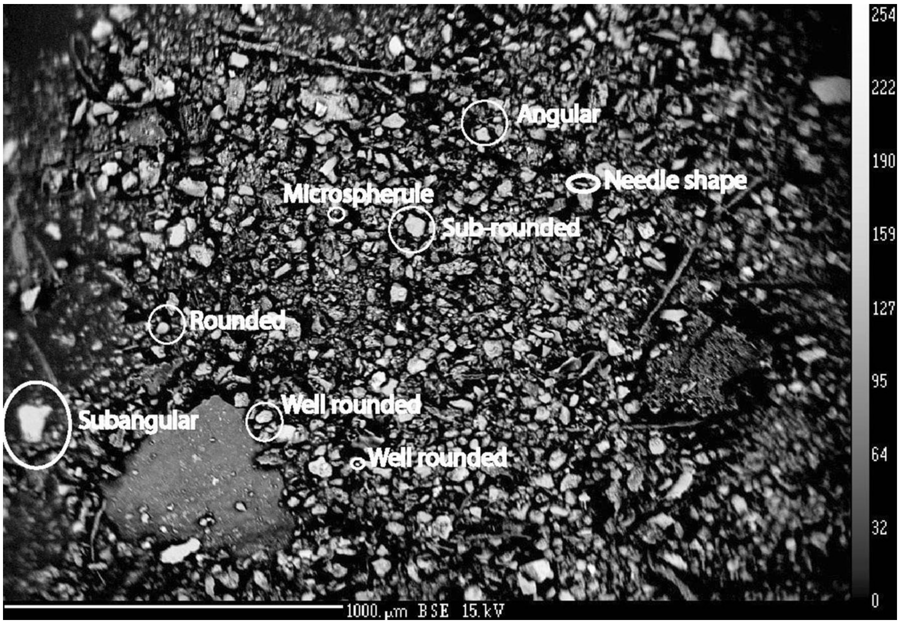

Fig. 5 BSE image showing various phases present in leaf dust samples. The variation in terms of grain shapes (angular, sub-angular, rounded, subrounded, well-rounded and needle shaped) is clearly visible and some microspherules are also present

REE geochemistry

The chondrite normalized (Sun & McDonough 1989) REE pattern of ten representative dust samples for 13 REEs is shown in Fig. 7 and the data is summarized in Table 4. The sample selection for REE analysis was based on their mass magnetic susceptibility variation (Table 2). The REE values of all the samples collected during the fog period are identical. They show a fractionated REE pattern with light REE (LREE) enrichment, nearly flat heavy REE (HREE) and a pronounced negative Eu anomaly (Eu/Eu*<1). All samples have a negative Eu anomaly (Eu/Eu*=0.15–0.17) with an average Eu/Eu* of 0.16. A positive Tb enrichment is also noted possibly due to the effect of standard (GSD-10) used for calibration by ICP-MS. The La_N/Yb_N values show un-differentiated fractionated pattern. Since the study area is situated close to the confluence of two major rivers (Ganga and Yamuna; Fig. 1) of India having large expanse of sandbars comprising sediments derived from the central India and the Himalayas mainly, a comparison of REE patterns with the rocks of Vindhyan Supergroup (Raza et al. 2012), Bundelkhand craton (Pati et al. 2008), and Himalayas (Rashid 2005) has been made. The REE contents and the normalized REE patterns of the rocks from Archean Bundelkhand craton (central India) and Kumaun Lesser Himalayas are found to be similar to the dust particles accumulated during the fog period in Allahabad, whereas, in general, the REE contents of sediments (Upper Vindhyan) though fractionated are relatively less in concentration.

Magnetic measurements

The magnetic measurements of the leaf dust are summarized in Table 2. The data show a moderate to high concentration of magnetic minerals in the analyzed samples. In case of total suspended particulate matter, the mean low-frequency magnetic susceptibility value is χ_{lf} 189.15×10^{-7} m kg^{-1} lying in the range between 16.08×10^{-7} and 848.10×10^{-7} m kg^{-1}, and the SIRM values vary from 928.6 to $81{,}554.1\times10^{-5}$ A m^2 kg^{-1} (Fig. 8). The SIRM is known to provide a rough measure in terms of concentration of all minerals having high magnetic remanence. The higher SIRM measurements are observed in heavy traffic areas (like Alopibagh tricrossing and Nehru Science Gate tricrossing) and the samples contain magnetite and ilmenite, the two ubiquitous ferromagnetic minerals. The lower SIRM values are observed in areas with less vehicular pollution (near Bharat Scouts and Guide School in front of Ganga Vihar). The raised χ_{lf} values in areas with high traffic volume (Bai Ka Bagh and Netram crossings, Katra) suggest the dominant contribution from Fe-bearing minerals in the mineral assemblage derived

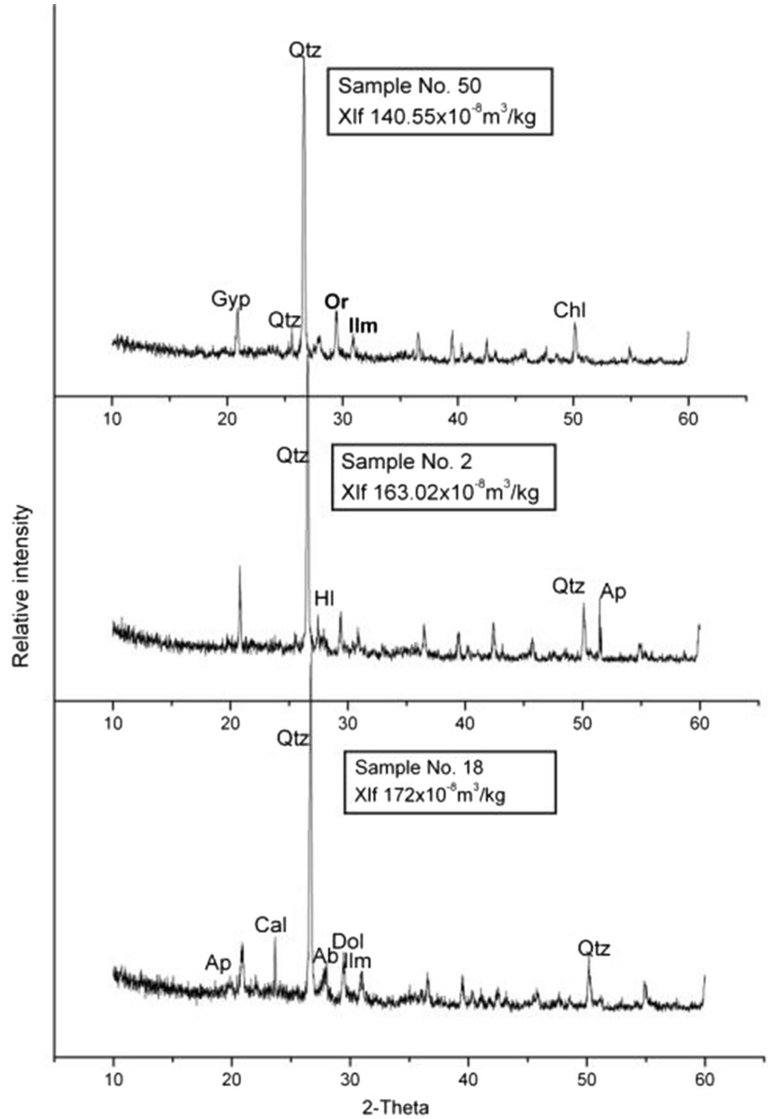

Fig. 6 The XRD patterns of the three representative samples showing quartz, biotite, dolomite, apatite minerals in the leaf dust sample

from vehicular exhaust (Thompson & Oldfield 1986). The SIRM value increases with an increase in the concentration of fine-size magnetic fractions (single domain; Bloemendal et al. 1992). The SIRM measurements also suggest that maximum concentrations of magnetic minerals occur in areas with high traffic density (Kushrubagh and Manmohan Park Gate intersections). The *S*-ratio is <90 % in less polluted area (Tularambagh side) indicating the presence of hematite. However, more magnetic minerals (100 %) are present in traffic junctions (George Town area). Overall the *S*-ratio shows a polymodal distribution in the entire sample area further supporting only localized minimal effect due to vehicular pollution in terms of the abundance of magnetic minerals. In general, the SIRM and *S*-ratio show the concentration of ferromagnetic constituents and fine grains of magnetic minerals as a magnetic proxy in the roadside leaf dust. The variation of χlf and SIRM in the study area are shown with the help of color contour spatial distribution maps (Fig. 9a and b), and they show minor variability in terms of χlf and SIRM, respectively. The quotient X_{ARM}/SIRM ($\overline{X}$ = 0.49 × 10^{-5} A m^{-1}; Table 2) may be used as an indicator of the relative importance of fine magnetic grains (Dunlop & Ozdemir 1997). The high *S*-ratio reflects convergence in which the magnetic properties are controlled by magnetite/maghemite, while the lower values indicate the greater contributions from anti-ferromagnetic minerals (Fig. 9c; Evans & Heller 2003) like hematite.

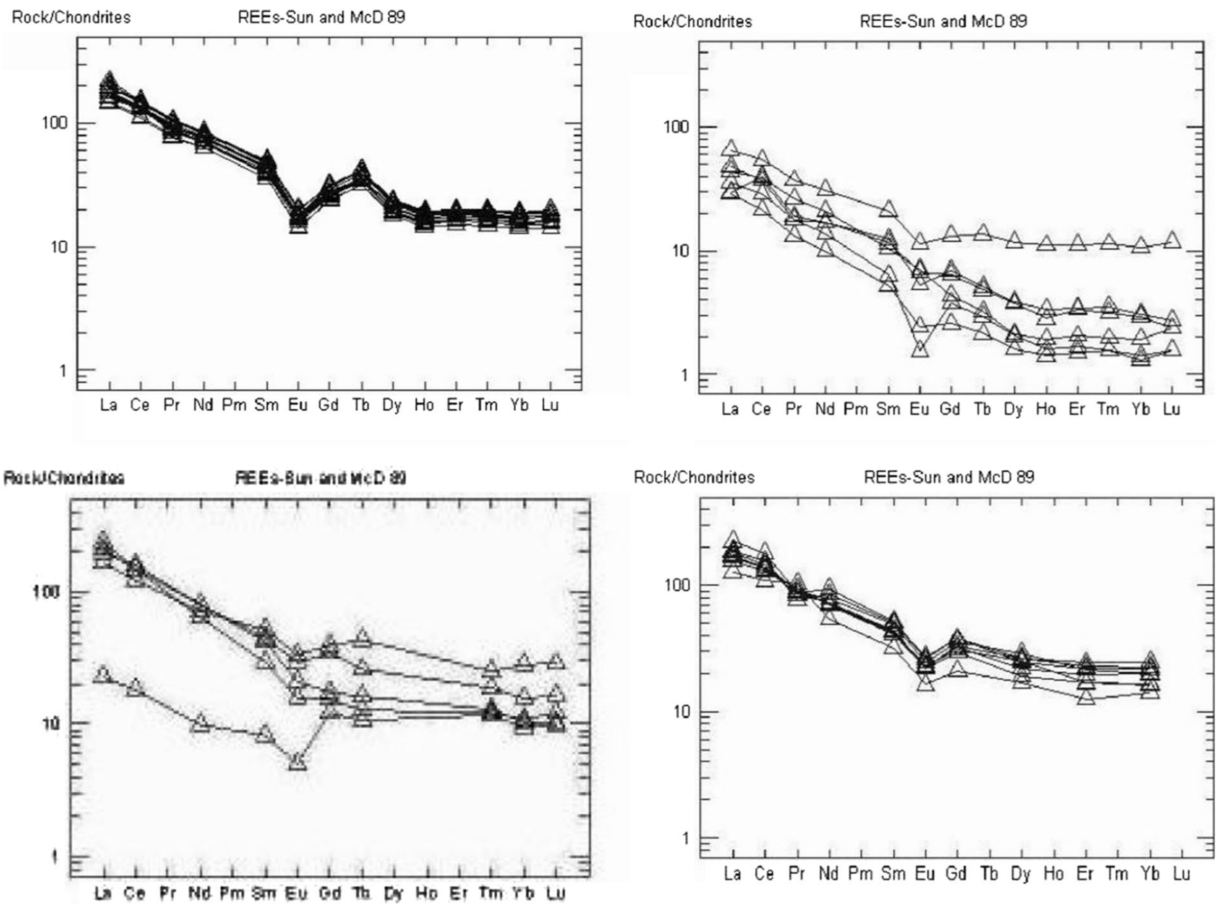

Fig. 7 Chondrite-normalized REE patterns and abundance of dust samples and some upper crustal assemblages of the region. **a** Sample source showing tree leaf particulate matter from north India, Allahabad. **b** Upper Vindhyan sedimentary rock (Raza et al. 2012). **c** Bundelkhand granitoids (Pati et al. 2008). **d** Mesoproterozoic clastic sedimentary rock from Kumaun Lesser Himalaya (Rashid 2005)

The mean frequency-dependent susceptibility (χ_{fd}%) value of dust samples is 13.06 %, which reveals the total concentration of SP grains, while the mean ARM value $14{,}752.07\times10^{-8}$ m^3 kg^{-1} shows the concentration of stable single domain (SSD) and fine pseudo-single domain (PSD) ferrimagnetic grains (Dunlop & Ozdemir 1997). The mean SIRM value $13{,}029.46\times10^{-5}$ A m^2 kg^{-1} indicates the average concentration of magnetic grains (Evans & Heller 2003).

Conclusions

The present study reports the physicochemical properties of accumulated dust during a well-documented regional fog period in the north India of 2010 from one of the strongly effected cities although the samples does not necessarily represent the fog condensates alone. The following conclusions are drawn from the present study:

(1) The dust collected during the fog period shows polymodal distribution in terms of their mass (0.10–3.74 g), and these values are relatively higher than those collected during premonsoon and postmonsoon months.
(2) The dust particulate size varies between 1.5 and 100 μm with 59.08 % lying within the size range for the fog condensates (0.23 and 20 μm).

Table 4 The rare earth element analyses of eight selected leaf dust samples carried out by ICP-MS technique is given below

Sample	6	8	12	23	35	36	43	45	Average	SD
La	46.97	41.83	43.71	49.42	51.94	41.84	35.54	45.78	44.62	5.10
Ce	93.64	80.97	83.52	90.7	93.05	9.89	69.96	90.13	85.23	8.18
Pr	10.14	8.80	9.26	9.97	10.18	8.90	7.46	9.72	9.30	0 .91
Nd	37.19	34.37	36.05	38.93	40.13	35.45	29.63	39.04	36.34	3.35
Sm	7.75	6.62	6.87	7.45	7.53	6.70	5.42	7.16	6.93	0.73
Eu	1.19	1.01	1.05	1.12	1.15	1.03	0.84	1.02	1.05	0.10
Gd	6.24	5.63	5.97	6.43	6.54	5.95	4.83	6.29	5.98	0.55
Tb	1.54	1.36	1.46	1.56	1.57	1.45	1.18	1.53	1.45	0.13
Dy	5.86	5.21	5.71	6.05	6.00	5.58	4.55	5.82	5.59	0.499
Ho	1.05	0.93	1.02	1.09	1.08	1.0	0.82	1.03	1.0	0.08
Er	3.17	2.87	3.12	3.33	3.32	3.06	2.50	3.20	3.07	0.27
Tm	0.50	0.44	0.47	0.51	0.50	0.46	0.38	0.49	0.46	0.042
Yb	3.08	2.80	2.95	3.24	3.22	2.92	2.38	3.14	2.96	0.28
Lu	0.50	0.45	0.46	0.50	0.50	0.46	0.36	0.51	0.46	0.05
Eu_N/Eu^*	0.17	0.17	0.16	0.16	0.16	0.16	0.16	0.15	0.16	0.16
La_N/Yb_N	15.25	14.93	14.81	15.25	16.13	14.32	14.93	14.57	15.07	18.21

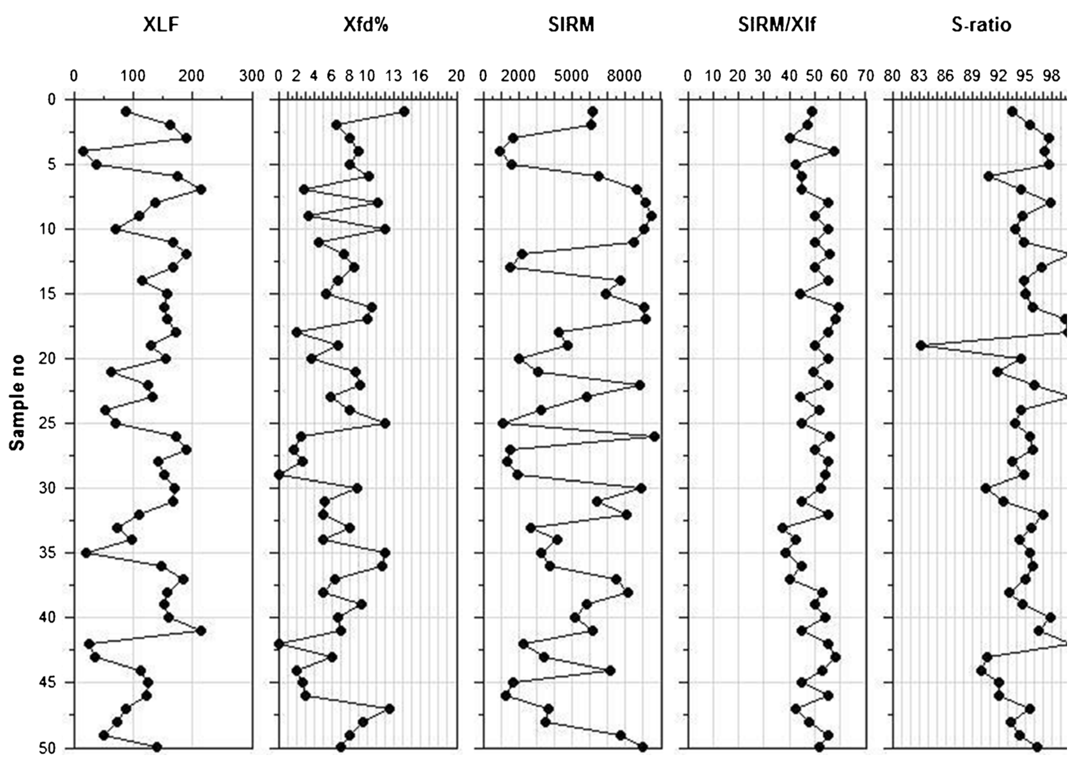

Fig. 8 Variation in different properties of magnetic coefficient in the leaf dust samples of the study area

Fig. 9 Contour map showing magnetic susceptibility, SIRM and *S*-ratios variations emphasizing the magnetic properties of leaf dust in the study area

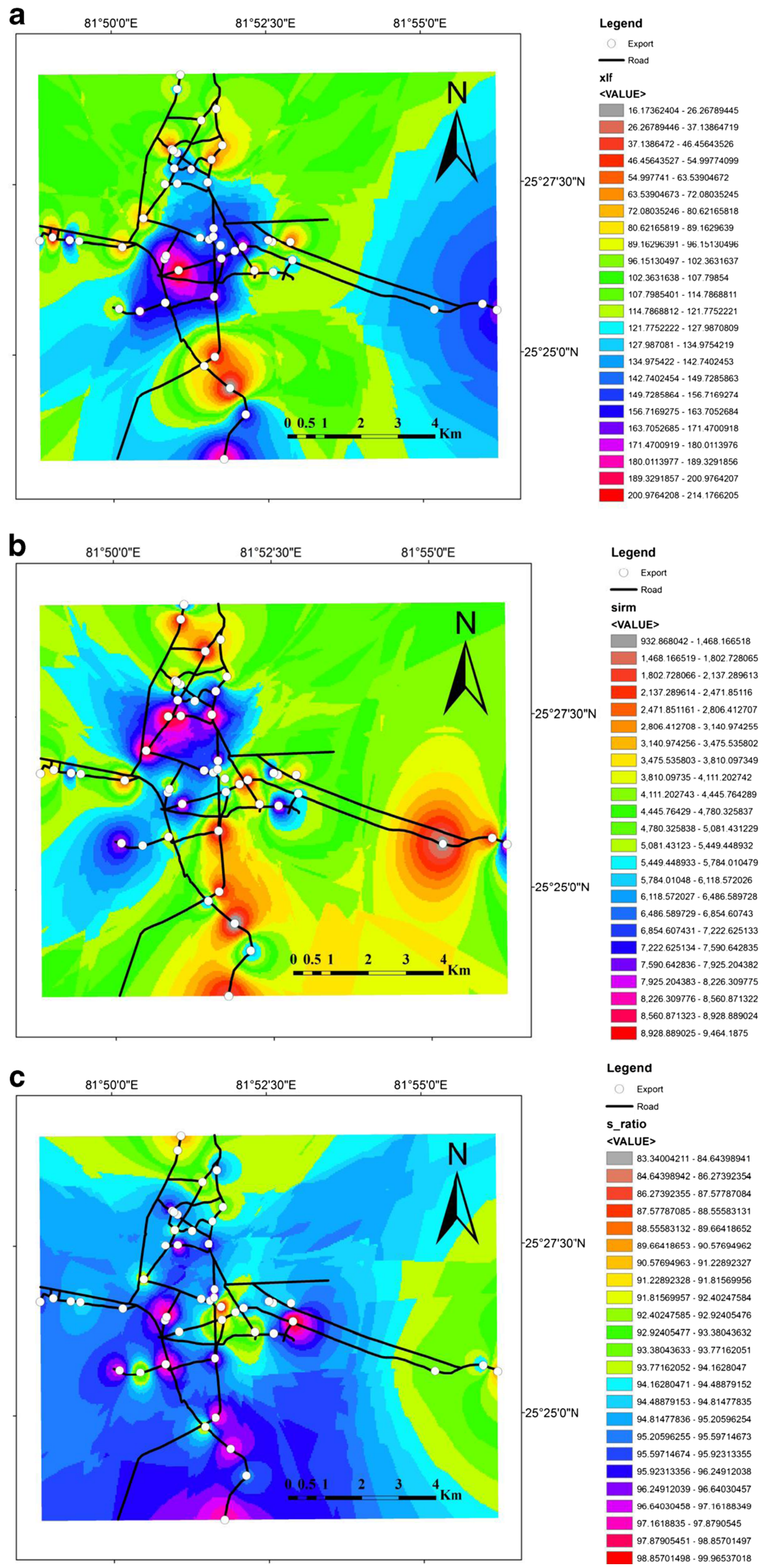

(3) The particulate shapes vary from subangular, angular, well-rounded, and needle-shaped, indicating their derivation from proximal as well as distal sources.
(4) The phases present in the samples include various inorganic (minerals like feldspar, quartz, mica, ilmenite, calcite, albite, magnetite, muscovite, and metallic phases), organic (husk and dried leaflets etc.), and other rare phases (glass and opaque spherules).
(5) The color of the dust samples observed during the fog period is strikingly different from the premonsoon and postmonsoon periods. The various hues of color have a direct bearing on their magnetic susceptibility values. The samples with darker hues have higher magnetic susceptibility.
(6) The REE patterns of dust samples exhibit identical fractionated patterns and are very similar to terrestrial upper crustal compositions. They show chemical similarity to cratonic and Himalayan lithologies with a possible contribution from the present-day point bar sediments of Ganga and Yamuna rivers.
(7) The magnetic measurements χ_{lf}, χ_{fd}%, SIRM, SIRM/χ_{lf}, and *S*-ratio suggest the presence of fine grained magnetite (with or without ilmenite) distributed uniformly over the entire study area and reflect localized anthropogenic contribution to the dust load.

Acknowledgments The authors gratefully acknowledge the Deputy Director General (NR), Geological Survey of India, Lucknow for the REE analyses, and the PLANEX, PRL, Department of Space, Government of India, (Ahmedabad) for electron probe microanalyzer analyses used in the present study, respectively. The GIS facilities kindly provided to JKP through the GRBM project, MoE&S, Government of India is also thankfully acknowledged.

References

Abdul-Razzaq, W., & Gautam, M. (2001). Discovery of magnetite in the exhausted material from a diesel engine. *Applied Physics Letters, 78*, 2018–2019.

Ali, K., Momin, G. A., Tiwari, S., Safai, P. D., Chate, D. M., & Rao, S. P. (2004). Fog and precipitation chemistry at Delhi, North India. *Atmospheric Environment, 38*, 4215–4222.

Biswas, K. F., Ghauri, B. M., & Husain, L. (2008). Gaseous and aerosol pollutants during fog and clear episodes in South Asian urban atmosphere. *Atmospheric Environment, 42*, 7775–7785.

Blaha, U., Sapkota, B., Apple, E., Stanjek, H., & Rosler, W. (2008). Micro-scale grain-size analysis and magnetic properties of coal-fired power plant fly ash and its relevance for environmental magnetic pollution studies. *Atmospheric Environment, 42*, 359–837.

Bloemendal, J., King, J. W., Hall, F. R., & Doh, S. J. (1992). Rock magnetism of Late Neogene and Pleistocene deep sediments: relationship to sediments source, genetic process and sediments lithology. *Journal of Geophysical Research, 97*, 4361–4375.

Cereceda, P., Larrain, H., Osses, P., Farías, M., & Egaña, I. (2008). The spatial and temporal variability of fog and its relation to fog oases in the Atacama Desert, Chile. *Atmospheric Research, 7*, 312–323.

Charlesworth, S. M., & Lees, J. A. (1997). The use of mineral magnetic measurements in polluted urban lakes and deposited dusts, Coventry, UK. *Physics and Chemistry of the Earth, 22*, 203–206.

Chaurasia, S., Sathiyamoorthy, V., Paul Shukla, B., Simon, B., Joshi, P. C., & Pal, P. K. (2011). Night time fog detection using MODIS data over Northern India. *Meteorological Applications, 18*(4), 483–494.

Chen, F. H., Yang, L. P., Wang, J. M., & Zhang, J. W. (1999). Study on atmospheric particulate pollution of Lanzhou using magnetic measurements. *Journal of Environmental Science, 11*(3), 73–77.

Choudhury, S., Rajpal, H., & Saraf, A. K. (2007). Mapping and forecasting of North Indian winter fog: an application of spatial technologies. *International Journal of Remote Sensing, 28*(16), 3649–3663.

Dunlop, D. J. (1973). Superparamagnetic and single domain threshold sizes in magnetite. *Journal of Geophysical Research, 78*, 780–1793.

Dunlop, D. J., & Ozdemir, O. (1997). *Rock magnetism: fundamentals and frontiers*. Cambridge: Cambridge University Press.

Evans, M. E., & Heller, F. (2003). *Environmental magnetism. Principles and applications of enviromagnetics* (p. 99). San Diego: Academic Press.

Flanders, P. J. (1994). Collection, measurements and analysis of airborne magnetic particulates from pollution in the environment. *Journal of Applied Physics, 5*, 931–5936.

Gautam, P., Blaha, U., & Apple, E. (2005). Magnetic susceptibility y of dust-loaded leaves as a proxy of traffic-related heavy metal pollution in Kathmandu City, Nepal. *Atmospheric Environment, 39*, 2201–2211.

Goddu, S. R., Appel, E., Jordanova, D., & Wehland, R. (2004). Magnetic properties of road dust from Vishakhapatnam (India)—relationship to industrial pollution and road traffic. *Physics and Chemistry of the Earth, 9*, 985–995.

Hanesch, H., & Scholger, R. (2002). Mapping of heavy metal loadings in soil by means of magnetic susceptibility measurements. *Environmental Geology, 42*, 857–870.

Hanesch, H., Scholger, R., & Rey, D. (2003). Mapping dust distribution around an industrial site by measuring parameters of tree leaves. *Atmospheric Environment, 37*, 5125–5133.

Hoffmann, V., Knab, M., & Appel, E. (1999). Magnetic susceptibility mapping of roadside pollution. *Journal of Geochemical Exploration, 6*, 13–326.

http://en.wikipedia.org/wiki/Allahabad. Accessed 20 December 2011.

http://IITRoorkee/IITRoorkee . Accessed on 20 December 2012.

Jenamani, R. K., & Tyagi, A. (2011). Monitoring fog at IGI Airport and analysis of its runway-wise spatio-temporal variations using meso-RVR network. *Current Science, 100*, 491–501.

Lorenzini, G., Grassi, C., Nali, C., Petiti, A., Loppi, S., & Tognotti, L. (2006). Leaves of *Pittosporum toriba* as indicators of airborne trace element and PM_{10} distribution in central Italy. *Atmospheric Environment, 40*, 4025–4036.

Lu, S. G., Bai, S. Q., & Xue, Q. F. (2007). Magnetic properties as indicators of heavy metals pollution in urban topsoils: a case study from the city of Luoyang, China. *Geophysical Journal International, 171*, 68–580.

Lu, S. G., Zheng, Y. W., & Bai, S. Q. (2008). A HRTEM/EDX approach to identification of the source of dust particles on urban tree leaves. *Atmospheric Environment, 42*, 431–6441.

Maher, B. A., Moore, C., & Matzka, J. (2007). Spatial variation in vehicle-derived metal pollution identified by magnetic and elemental analysis of roadside tree leaves. *Atmospheric Environment, 42*, 364–373.

Moreno, E., Sagnotti, L., Turell, J. D., Winkler, A., & Cascella, A. (2003). Biomonitoring of traffic air pollution in Rome using magnetic properties of tree leaves. *Atmospheric Environment, 7*, 2967–2977.

Muxworthy, A. R., Schmidbauer, E., & Petersen, N. (2002). Magnetic properties and Mossbauer spectra of urban atmospheric particulate matter: a case study from Munich, Germany. *Geophysical Journal International, 150*, 558–570.

Oldfield, F., Hunt, A., Jones, M. D. H., Chester, R., Dearing, J. A., Olsson, L., et al. (1985). Magnetic differentiation of atmospheric dusts. *Nature, 317*, 516–518.

Pant, V., Deshpande, C. G., & Kamra, A. K. (2010). Changes in concentration and size distribution of aerosols during fog over the south Indian Ocean. *Journal of Earth System Science, 119*, 479–487.

Pati, J. K., Reimold, W. U., Koeberl, C., & Pati, P. (2008). The Dhala structure, Bundelkhand Craton, Central India—eroded remanant of a large Paleoproterozoic impact structure. *Meteoritics and Planetary Science, 43*, 1383–1398.

Petrovsky, E., & Ellwood, B. B. (1999). Magnetic monitoring of pollution of air, land and water. In B. A. Maher & R. Thomposon (Eds.), *Quaternary climates, environments and magnetism* (pp. 279–322). Cambridge: Cambridge University Press.

Power, L. A., Worsley, T. A., & Booth, C. (2009). Magneto-biomonitoring of intra-urban spatial variations of particulate matter using tree leaves. *Environmental Geochemistry and Health, 31*, 315–325.

Prajapati, S. K., & Tripathi, B. D. (2008). Management of hazardous road derived respirable particulates using magnetic properties of tree leaves. *Environmental Monitoring and Assessment, 139*, 351–354.

Prasad, A. K., & Singh, R. P. (2007). Comparison of MISR-MODIS aerosol optical depth over the Indo-Gangetic basin during the winter and summer seasons (2000–2005). *Remote Sensing of Environment, 107*, 109–119.

Rashid, S. A. (2005). The geochemistry of Mesoproterozoic clastic sedimentary rocks from the Rautgara Formation, Kumaun Lesser Himalaya: implications for provenance, mineralogical control and weathering. *Current Science, 88*(11), 1832–1836.

Raza, M., Khan, A., Bhardwaj, V. R., & Rais, S. (2012). Geochemistry of Mesoproterozoic sedimentary rocks of upper Vindhyan Group, southeastern Rajasthan and implications for weathering history, composition and tectonic setting of continental crust in the northern part of Indian shield. *Journal of Asian Earth Sciences, 48*, 160–172.

Saraf, A. K., Bora, A. K., Das, J., Rawat, V., Sharma, K., & Jain, S. K. (2011). Winter fog over the Indo-Gangetic Plains: mapping and modeling using remote sensing and GIS. *Natural Hazards, 201*(58), 199–220.

Shu, J., Dearing, J. A., Morse, A. P., Yu, L. Z., & Li, C. Y. (2000). Magnetic properties of daily sampled total suspended particulates in Shanghai. *Environmental Science & Technology, 34*, 2393–2400.

Singh, V. K., Gupta, T., Tripathi, S. N., Jariwala, C., & Das, U. (2011). Experimental study of the effects of environmental and fog condensation nuclei parameters on the rate of fog formation and dissipation using a new laboratory scale fog generation facility. *Aerosol and Air Quality Research, 11*, 140–154.

Spassov, S., Egli, R., Heller, F., Nourgaliev, D. K., & Hannam, J. (2004). Magnetic quantification of urban pollution sources in atmospheric particulate matter. *Geophysical Journal International, 59*, 555–564.

Sun, S. S., & McDonough, W. F. (1989). Chemical and isotopic systematics of oceanic basalts: implications for mantle composition and processes. *Geological Society London Special Publications, 42*, 313–345.

Thompson, R., & Oldfield, F. (1986). Environmental magnetism. London: Allen & Unwin. ISBN-0–04–538003, 277.

Tiwari, S., Payra, S., Mohan, M., Verma, S., & Bisht, D. S. (2011). Visibility degradation during foggy period due to anthropogenic urban aerosol at Delhi, India. *Atmospheric Pollution Research, 2*, 116–120.

Tomaˇsevi'c, M., Vukmirovic', Z., Rajsˇic', S., Tasic', M., & Stevanovic', B. (2005). Characterization of trace metal particles deposited on some deciduous tree leaves in an urban area. *Chemosphere, 61*, 753–760.

Wong, C. S. L., Li, X. D., & Thornton, I. (2006). Urban environmental geochemistry of trace metals. *Environmental Pollution, 142*, 1–16.

Yang, L. P., & Chen, F. H. (2002). Chemical characteristics of atmospheric dust in Lanzhou. *Acta Scientiae Circumstantiae, 22*(4), 499–502.